Applied Physics Letters

Wurtzite BAlN and BGaN alloys for heterointerface polarization engineering

Cite as: Appl. Phys. Lett. **111**, 222106 (2017); https://doi.org/10.1063/1.5008451
Submitted: 06 October 2017 . Accepted: 14 November 2017 . Published Online: 30 November 2017

Kaikai Liu, Haiding Sun, Feras AlQatari, Wenzhe Guo, Xinwei Liu, Jingtao Li, Carlos G Torres Castanedo, and Xiaohang Li

Wurtzite BAlN and BGaN alloys for heterointerface polarization engineering

Kaikai Liu, Haiding Sun, Feras AlQatari, Wenzhe Guo, Xinwei Liu, Jingtao Li, Carlos G Torres Castanedo, and Xiaohang Li
King Abdullah University of Science and Technology (KAUST), Advanced Semiconductor Laboratory, Thuwal 23955-6900, Saudi Arabia

(Received 6 October 2017; accepted 14 November 2017; published online 30 November 2017)

The spontaneous polarization (SP) and piezoelectric (PZ) constants of $B_xAl_{1-x}N$ and $B_xGa_{1-x}N$ ($0 \le x \le 1$) ternary alloys were calculated with the hexagonal structure as reference. The SP constants show moderate nonlinearity due to the volume deformation and the dipole moment difference between the hexagonal and wurtzite structures. The PZ constants exhibit significant bowing because of the large lattice difference between binary alloys. Furthermore, the PZ constants of $B_xAl_{1-x}N$ and $B_xGa_{1-x}N$ become zero at boron compositions of ~87% and ~74%, respectively, indicating non-piezoelectricity. The large range of SP and PZ constants of $B_xAl_{1-x}N$ (BAlN) and $B_xGa_{1-x}N$ (BGaN) can be beneficial for the compound semiconductor device development. For instance, zero heterointerface polarization ΔP can be formed for BAlN and BGaN based heterojunctions with proper B compositions, potentially eliminating the quantum-confined Stark effect for c-plane optical devices and thus removing the need of non-polar layers and substrates. Besides, large heterointerface polarization ΔP is available that is desirable for electronic devices. *Published by AIP Publishing.*
https://doi.org/10.1063/1.5008451

As an emerging member of the III-nitride family, wurtzite (WZ) $B_xAl_{1-x}N$ alloys ($0 \le x \le 1$) (hereafter BAlN) possess a large range of refractive indexes and lattice constants.[1,2] Recently, single-phase WZ BAlN layers with a relatively large boron (B) composition (14.4%) and thickness (100 nm) have been demonstrated epitaxially.[3,4] In addition, the band alignment and microstructure of the BAlN/AlGaN heterojunction have been studied, indicating large conduction band offset desirable for optical and electronic device applications.[5] Similarly, WZ $B_xGa_{1-x}N$ alloys ($0 \le x \le 1$) (hereafter BGaN) have exhibited a wide range of bandgaps and lattice constants that may provide vast opportunities for device applications.[6,7]

III-nitrides can exhibit strong spontaneous polarization (SP) and piezoelectric (PZ) polarization. The resulting heterointerface polarization can impact the device operation considerably. For instance, the quantum-confined Stark effect (QCSE) caused by the heterointerface polarization in the quantum well (QW) of light emitters can reduce radiative recombination rates and shift emission wavelength.[8] In addition, the heterointerface polarization can lead to strong carrier confinement and thus formation of two-dimensional electron gas (2DEG), which enables the operation of a high electron mobility transistor (HEMT).[9,10]

Recently, a significant increase in the UV spontaneous emission rate from the B-containing QW structure was reported by Park *et al.*, which resulted from the decrease in the internal polarization field through B incorporation.[11,12] However, the polarization constants of the B-containing materials utilized by the studies were based on the linear interpolation of the binary material constants.[11,12] The linear interpolation may not be accurate, though, as Bernardini and Fiorentini have shown considerable nonlinearity in both SP and PZ constants of AlGaN, InGaN, and AlInN versus the respective material composition.[13] Therefore, accurate SP and PZ constants of the BAlN and BGaN ternary alloys are crucial. Unfortunately, they are still absent. In this work, the SP and PZ constants of BAlN and BGaN alloys were studied theoretically. The constants have considerable bowing with respect to the B composition. Potential heterojunctions and device applications comprising these alloys are discussed.

The calculations were carried out by the Vienna *ab initio* Simulation Package (VASP) software with generalized gradient approximation (GGA) as the exchange-correlation functional. The previous and our studies show that the polarization properties calculated based on GGA are in good agreement with the ones based on local density approximation (LDA) and hybrid functionals such as Heyd, Scueria, and Ernzerhof (HSE).[14,15] The ionic potentials were represented by the projector augmented wave method.[16] The calculations were performed on bulk primitive cells with a $6 \times 6 \times 6$ Monkhorst-Pack[17] k-point mesh to sample the Brillouin zone at a cutoff energy of 520 eV for the plane-wave basis set. In the structural optimization process, the primitive cells were fully relaxed with the Hellman-Feynman force of less than 0.02 eV Å^{-1}, from which the lattice constants and internal parameter deviation $\Delta u = u - u_{ideal}$ ($u_{ideal} = 0.375$) were obtained. The SP and the dipole change Δp were evaluated using the Berry phase approach within the context of the modern polarization theory suggested by King-Smith, Vanderbilt, and Resta.[18,19] Dreyer *et al.* recently show that the layered hexagonal (H) structure rather than the zincblende (ZB) structure be the reference crystal structure for the accuracy of the SP constants.[20] The H structure was thus utilized as the reference structure in this study. The SP constant was calculated by

$$P_{sp}^{(H\,Ref)} = \Delta p/\Omega, \tag{1}$$

where Ω and Δp are the cell volume and the dipole change, respectively. The structural parameters and SP constants of WZ GaN, AlN, and BN binary alloys were computed and are presented in Table I, which are in good agreement with previous studies.[20,21]

TABLE I. Structural parameters and SP constants of WZ GaN, AlN, and BN.

		a (Å)	c (Å)	Δu (10^{-3})	$P_{sp}^{(H\,ref)}$ (C/m^2)
GaN	This work	3.182	5.180	1.7	1.339
	Ref. 20	3.205	5.200	2.0	1.312
AlN	This work	3.113	4.981	7.3	1.333
	Ref. 20	3.099	4.959	7.0	1.351
BN	This work	2.528	4.180	0.6	2.118
	Ref. 21	2.520	4.170	…	2.174

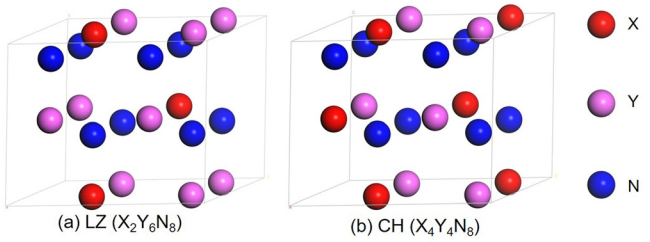

FIG. 1. 16-atom supercells of the (a) LZ-like (25%, 75%) and (b) CH-like (50%) structures. X and Y can be B, Al, or Ga atoms.

For ternary alloys, the cations are randomly distributed among cation sites, while anion sites are always occupied by nitrogen atoms. It was observed experimentally that different types of ordering exist in III-nitride ternary alloys.[22] A previous study on SP and PZ constants of conventional III-nitride ternary alloys including AlGaN, InGaN, and AlInN shows that the SP from supercells with different orderings of cation atoms can differ considerably.[13] The special quasirandom structure (SQS) can efficiently represent the microscopic structure of a random alloy in periodic conditions.[23] But the SQS can only apply for the case of ternary alloys with two cations having equal composition (i.e., 50% each).[13] On the other hand, the chalcopyrite-like (CH, in Fig. 1) structure defined by two cations of one species and two cations of the other species surrounding each anion (hence 50%) and the luzonite-like structure (LZ, in Fig. 1) defined by three cations of one species and one cation of the other species surrounding each anion (hence 25% or 75%) can well represent the microscopic structure of a random alloy for the calculation of the SP and PZ constants.[13] Thus, B compositions of 0, 25%, 50%, 75%, and 100% were employed for BAlN and BGaN, while the rest of the compositions were covered by quadratic regression.

Specifically, the 16-atom supercells of the CH-like (50%) and LZ-like (25%, 75%) structures were adopted. The calculation configuration was the same as those used for binary alloys. The CH-like or LZ-like supercells were optimized, from which the lattice constants of BAlN and BGaN with different B compositions were found to be consistent with the previous reports with small bowing parameters, as shown in Fig. 2.[1,6] By applying the second-order polynomial fitting, the lattice constants are as follows:

$$a(B_xAl_{1-x}N) = -0.157x^2 - 0.408x + 3.109\,(\text{Å}), \quad (2)$$

$$c(B_xAl_{1-x}N) = 0.119x^2 - 0.905x + 5.186\,(\text{Å}), \quad (3)$$

$$a(B_xGa_{1-x}N) = -0.101x^2 - 0.529x + 3.176(\text{Å}), \quad (4)$$

$$c(B_xGa_{1-x}N) = 0.057x^2 - 1.042x + 5.186(\text{Å}). \quad (5)$$

The dipole change of the supercells along the adiabatic transformation from the H to WZ structure was then calculated [Fig. 3(b)]. Subsequently, the SP versus different B compositions was obtained [Fig. 3(a)]. A moderate nonlinear behavior of the SP of BAlN and BGaN is observed which is consistent with those of InGaN, AlGaN, and AlInN.[13] The SP constants can be fitted by the following equations:

$$P_{sp}^{(H\,Ref)}(B_xAl_{1-x}N) = 0.629x^2 + 0.122x + 1.354, \quad (6)$$

$$P_{sp}^{(H\,Ref)}(B_xGa_{1-x}N) = 0.438x^2 + 0.314x + 1.354. \quad (7)$$

To understand the physical origin of the SP nonlinearity, Bernardini *et al.* modeled the SP nonlinearity of the ternary alloy SP with the ZB reference from the volume deformation by the linear interpolation of the SP of the binary III-nitrides in their ideal WZ structure as a function of the lattice constants $a(x)$ and hence under hydrostatic compression or dilution state as described by the following equation:[13]

$$P_{sp}(A_xB_{1-x}N) = xP_{sp}^{a(x)}(AN) + (1-x)P_{sp}^{a(x)}(BN). \quad (8)$$

In the Bernardini's model, volume deformation of the ternary alloys and the resultant electronic property related to the unit cell dipole moment are included. In this study with the H structure being the reference, the calculation and analysis are based on Eq. (1), $P_{sp}^{(H\,Ref)} = \Delta p/\Omega$. Thus, the SP nonlinearity can be decomposed into two distinct aspects: (1) the volume deformation or lattice variation due to B incorporation into binaries; and (2) the dipole moment difference between the H and WZ structure alloys due to the alternation of cation-anion bond lengths caused by the B incorporation and different chemical identities. Figure 3(b) shows the dipole change

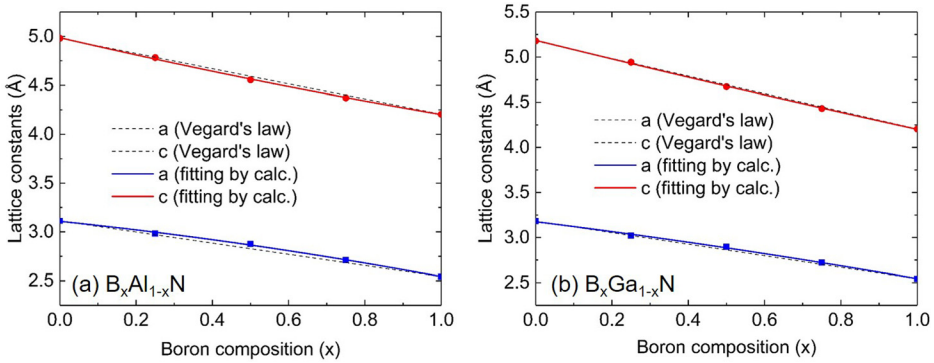

FIG. 2. Calculated lattice constants versus the B composition of WZ (a) BAlN and (b) BGaN.

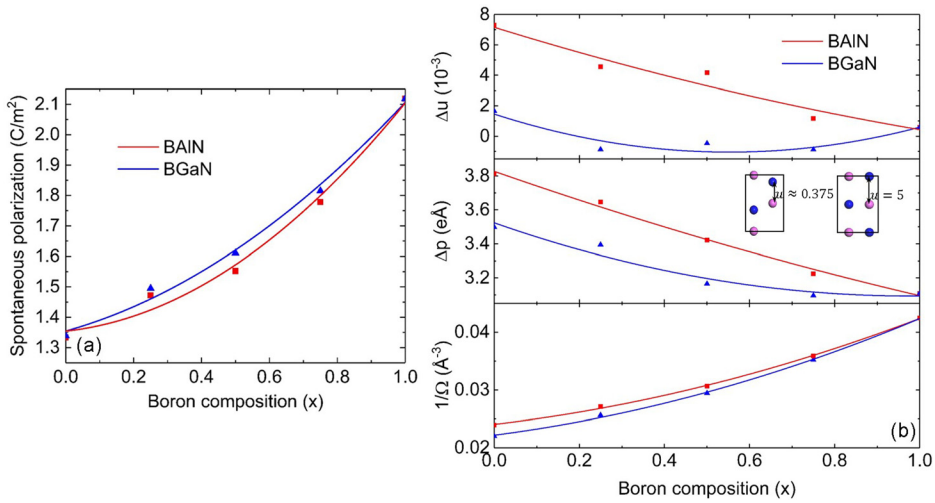

FIG. 3. (a) SP versus the B composition of BAlN and BGaN. (b) Δu measures the internal parameter deviation from the ideal crystal structure; dipole change Δp per unit cell from the H to WZ structure while the internal parameter u changes from $\sim$0.375 to 0.5; $1/\Omega$ shows the change of cell volume.

per unit cell of the ternary alloys from the H to the optimized WZ structure. The dipole change exhibits the same trend as the internal parameter deviation Δu which characterizes the internal strain effect. On the other hand, the dipole change of BAlN and BGaN alloys decreases with the higher B composition, while the SP increases as a result of the reduction of lattice constants and thus the increase of $1/\Omega$ with higher B incorporation. This shows that the main contribution of the SP nonlinearity is from the volume deformation according to Eq. (1).

The SP constants are not adequate to evaluate polarization-induced effects such as interface charge and built-in polarization field in WZ III-nitride heterojunctions. Due to the lattice mismatch, PZ polarization can be induced by applied strain (ϵ_3 or ϵ_1) and crystal deformation, which is characterized by mainly two PZ constants, e_{33} and e_{31}, given by the following equations:

$$e_{33} = e_{33}^{(0)} + e_{33}^{(IS)} = \left.\frac{\partial P_3}{\partial \epsilon_3}\right|_u + \left.\frac{\partial P_3}{\partial u}\right|_{\epsilon_3} \frac{du}{d\epsilon_3} = e_{33}^{(0)} + \frac{2e}{a^2} Z^* \frac{du}{d\epsilon_3}, \tag{9}$$

$$e_{31} = e_{31}^{(0)} + e_{31}^{(IS)} = \left.\frac{\partial P_3}{\partial \epsilon_1}\right|_u + \left.\frac{\partial P_3}{\partial u}\right|_{\epsilon_1} \frac{du}{d\epsilon_1} = e_{31}^{(0)} + \frac{2e}{a^2} Z^* \frac{du}{d\epsilon_1}. \tag{10}$$

The PZ constants, also referred to as the relaxed terms, comprise two parts: $e_{33}^{(0)}$ is the clamped-ion term obtained with the fixed internal parameter u and $e_{31}^{(IS)}$ is the internal-strain term from the bond alteration with external strain. P_3 is the macroscopic polarization along the c-axis, u is the internal parameter, Z^* is the zz component of the Born effective charge tensor, e is the electronic charge, and a is the a lattice constant. Besides, the PZ constants calculated here are proper according to Dreyer *et al.*[20]

For the PZ constants, we remained to use GGA in the DFT calculation. The density functional perturbation theory (DFPT)[24] was applied to calculate the PZ constants. The calculated PZ constants of BAlN and BGaN are shown in Fig. 4(a) and (b), respectively. By the second-order polynomial fitting, they can be described by the following equations:

$$e_{33}(B_xAl_{1-x}N) = -4.036x^2 + 1.684x + 1.547, \tag{11}$$

$$e_{31}(B_xAl_{1-x}N) = 1.762x^2 - 0.900x - 0.602, \tag{12}$$

$$e_{33}(B_xGa_{1-x}N) = -2.189x^2 + 0.817x + 0.539, \tag{13}$$

$$e_{31}(B_xGa_{1-x}N) = 0.981x^2 - 0.401x - 0.310. \tag{14}$$

Both e_{33} and e_{31} of BAlN and BGaN demonstrate significant bowing. The nonlinear piezoelectricity in WZ III-nitrides has been reported where the PZ polarization shows strong dependence on the strain caused by the lattice mismatch at the heterojunction interface.[25,26] To explain the physical origin of the PZ nonlinearity, Bernardini *et al.* incorporated the stain-dependent PZ nonlinearity of the bulk binary III-nitrides into the composition-dependent PZ nonlinearity of the ternary alloys by considering the ternary alloys as the linear combination of the strained, compressed, or tensile binary III-nitrides.[13] According to this model, the binary

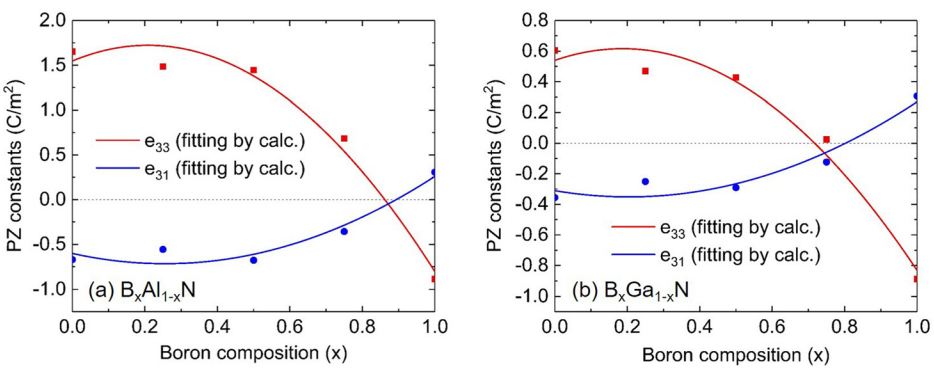

FIG. 4. PZ constants versus the B composition of (a) BAlN and (b) BGaN.

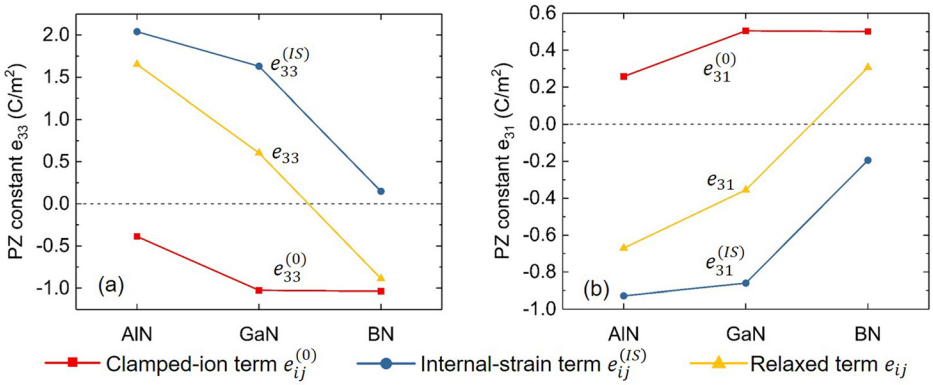

FIG. 5. Clamped-ion, internal-strain, and relaxed terms of the PZ constants (a) e_{33} and (b) e_{31} of WZ AlN, GaN, and BN.

III-nitrides experience a much larger lattice mismatch for BAlN and BGaN, up to ~25% (between BN and GaN), because of the much smaller lattice of BN compared to those of AlN and GaN. This is responsible for the large nonlinearity of the PZ constants of BAlN and BGaN. Furthermore, the PZ constants of BAlN and BGaN can turn zero at high B compositions of ~87% and ~74% when both e_{33} and e_{31} simultaneously become nearly zero, respectively, as shown in Figs. 4(a) and 4(b). It is noted that because of the large bowing parameters, the zeroing of the PZ constants happens at a much higher B composition than 50% as predicted by Vegard's law.

In Fig. 5, we computed the clamped-ion and internal-strain terms of AlN, GaN, and BN. It is noted that $e_{33}^{(0)}$ and $e_{31}^{(0)}$ are always negative and positive, respectively. Additionally, BN has much smaller $e_{33}^{(IS)}$ and $e_{31}^{(IS)}$ compared to AlN and GaN, which leads to negative e_{33} and positive e_{31} of BN. Therefore, the zero PZ constants result from negative e_{33} and positive e_{31} of BN, while AlN and GaN both possess positive e_{33} and negative e_{31}. Thus, the combination of AlN, GaN, and BN forming ternary alloys gives rise to the zero piezoelectricity.

The polarization properties of BAlN and BGaN can offer opportunities for device design when forming metal- or N-polar heterojunctions with conventional III-nitrides including GaN, AlN, and their alloys. Moreover, they can form heterojunctions mutually by growing BAlN on the relaxed BGaN substrate or vice versa with varying B compositions. The epitaxial layer is presumably strained to the substrate for Fig. 6, but similar plots can be made given the degree of lattice relaxation as well. Thus, we can estimate the polarization difference ΔP at the c-plane heterointerface

$$\Delta P\,(x,y) = [P_{sp}^{(epi)}(x) - P_{sp}^{(sub)}(y)] + P_{pz}^{(epi)}\,(x,y), \tag{15}$$

$$P_{pz}^{(epi)}(x,y) = 2\left[e_{31}^{(epi)}(x) - P_{sp}^{(epi)}(x) - \frac{C_{13}^{(epi)}(x)}{C_{33}^{(epi)}(x)}e_{33}^{(epi)}(x)\right] \times \frac{a^{(sub)}(y) - a^{(epi)}(x)}{a^{(epi)}(x)}. \tag{16}$$

Here, $e_{31}^{(epi)}(x)$ and $e_{33}^{(epi)}(x)$ are the proper PZ constants[20] of the epitaxial layer, $C_{13}^{(epi)}(x)$ and $C_{33}^{(epi)}(x)$ are the elastic constants of the epitaxial layer based on the linear interpolation of the binary values,[14] x is the B composition of the epitaxial layer, and y is the B composition of the substrate. $\Delta P\,(x,y)$ is

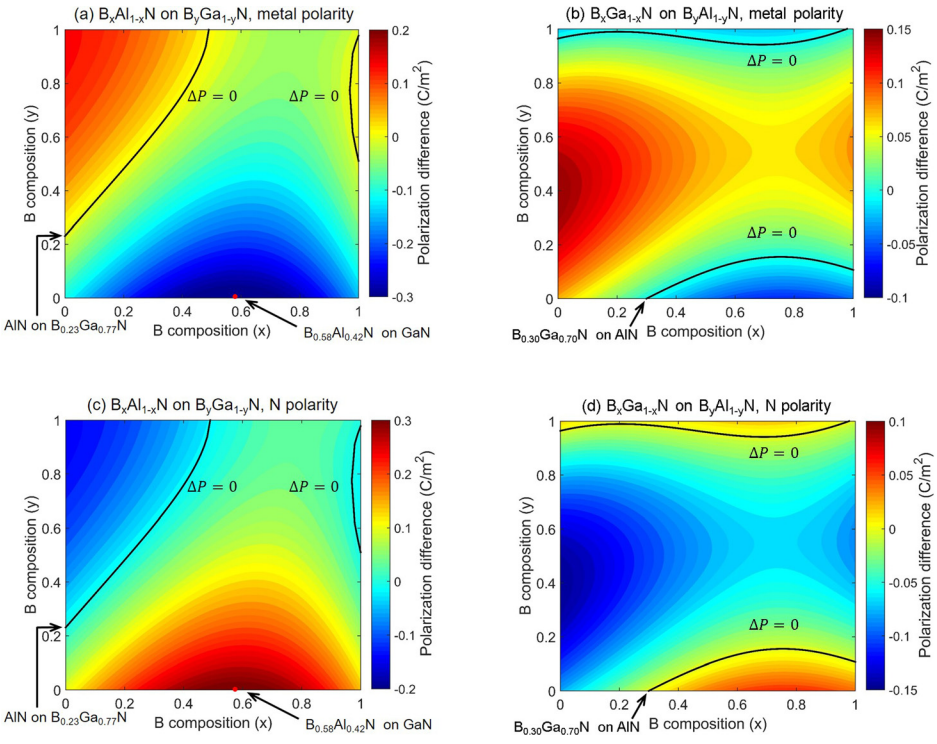

FIG. 6. The estimated heterointerface polarization difference ΔP of metal-polar and N-polar BAlN/BGaN and BGaN/BAlN heterojunctions. Black lines indicate zero ΔP. ΔP being positive means that there is negative polarization charge accumulation at the heterointerface.

plotted in Fig. 6. The black curves represent zero heterointerface polarization difference ΔP. They indicate QCSE-free heterojunctions desirable for *c*-plane optical devices.[8] The zero polarization difference ΔP is caused by the cancellation of the SP and PZ terms in Eq. (15) at certain compositions of the epitaxial layer and the substrate, such as the $B_{0.30}Ga_{0.70}N$-on-AlN heterojunction in Figs. 6(b) and (d) as well as many others along the black curves in Figs. 6(a)–6(d). On the other hand, large polarization differences can be found when moving away from the black curves in Figs. 6(a)–6(d) that are desirable for electronic devices. For instance, the metal-polar $B_{0.58}Al_{0.42}N$-on-GaN heterojunction can have a large polarization difference up to $-0.3\,C/m^2$ [Fig. 6(a)]. However, it is noted that the PZ constants can be strain-dependent which is not considered in Figs. 6(a)–6(d).[27,28] Thus, the polarization contours in Fig. 6 may possess deviation when the lattice mismatch is too large. In summary, the SP and PZ constants of BAlN and BGaN have been calculated. Moderate and strong nonlinearity of the SP and PZ constants were found with respect to the B composition, respectively. The nonlinearity of the SP constants is caused by volume deformation and difference of dipole moment between the H and WZ structures. The nonlinearity of the PZ constants is due to the large lattice difference between the binary alloys. BAlN and BGaN can turn non-PZ at high B compositions of 87% and 74%, respectively, due to opposite signs of PZ constants of the binary alloys. The large range of SP and PZ constants of BAlN and BGaN can benefit development of optical and electronic heterojunction devices when forming heterojunctions with conventional III-nitrides. Moreover, the BAlN/BGaN and BGaN/BAlN heterojunctions can lead to from zero to large heterointerface polarization difference desirable for optical and electronic devices, respectively.

The KAUST authors would like to acknowledge the support of GCC Research Program REP/1/3189-01-01 and KAUST Baseline Fund BAS/1/1664-01-01.

[1]M. Zhang and X. Li, Phys. Status Solidi B **254**, 1600749 (2017).
[2]M. Abid, T. Moudakir, G. Orsal, S. Gautier, A. E. Naciri, Z. Djebbour, J. H. Ryou, G. Patriarche, L. Largeau, H. J. Kim, Z. Lochner, K. Pantzas, D. Alamarguy, F. Jomard, R. D. Dupuis, J. P. Salvestrini, P. L. Voss, and A. Ougazzaden, Appl. Phys. Lett. **100**, 051101 (2012).
[3]X. Li, S. Wang, H. Liu, F. A. Ponce, T. Detchprohm, and R. D. Dupuis, Phys. Status Solidi B **254**, 1600699 (2017).
[4]S. Wang, X. Li, A. M. Fischer, T. Detchprohm, R. D. Dupuis, and F. A. Ponce, J. Cryst. Growth **475**, 334 (2017).
[5]H. Sun, Y. Park, K. H. Li, C. G. T. Castanedo, A. S. Alowayed, T. Detchprohm, R. D. Dupuis, and X. Li, Appl. Phys. Lett. **111**, 122106 (2017).
[6]A. Said, M. Debbichi, and M. Said, Optik **127**, 9212 (2016).
[7]A. Ougazzaden, S. Gautier, T. Moudakir, Z. Djebbour, Z. Lochner, S. Choi, H. J. Kim, J. H. Ryou, R. D. Dupuis, and A. A. Sirenko, Appl. Phys. Lett. **93**, 083118 (2008).
[8]F. Wu, H. Sun, I. A. Ajia, I. S. Roqan, D. Zhang, J. Dai, C. Chen, Z. C. Feng, and X. Li, J. Phys. D: Appl. Phys. **50**, 245101 (2017).
[9]O. Ambacher, J. Smart, J. R. Shealy, N. G. Weimann, K. Chu, M. Murphy, W. J. Schaff, L. F. Eastman, R. Dimitrov, L. Wittmer, M. Stutzmann, W. Rieger, and J. Hilsenbeck, J. Appl. Phys. **85**, 3222 (1999).
[10]O. Ambacher, B. Foutz, J. Smart, J. R. Shealy, N. G. Weimann, K. Chu, M. Murphy, A. J. Sierakowski, W. J. Schaff, L. F. Eastman, R. Dimitrov, A. Mitchell, and M. Stutzmann, J. Appl. Phys. **87**, 334 (2000).
[11]S. H. Park, Opt. Express **23**, 3623 (2015).
[12]S. H. Park and D. Ahn, IEEE Photonics Technol. Lett. **28**, 2153 (2016).
[13]F. Bernardini and V. Fiorentini, Phys. Rev. B **64**, 085207 (2001).
[14]A. Zoroddu, F. Bernardini, P. Ruggerone, and V. Fiorentini, Phys. Rev. B **64**, 045208 (2001).
[15]F. Bernardini, V. Fiorentini, and D. Vanderbilt, Phys. Rev. B **63**, 193201 (2001).
[16]P. E. Blochl, Phys. Rev. B **50**, 17953 (1994).
[17]H. J. Monkhorst and J. D. Pack, Phys. Rev. B **13**, 5188 (1976).
[18]R. D. Kingsmith and D. Vanderbilt, Phys. Rev. B **47**, 1651 (1993).
[19]R. Resta, Rev. Mod. Phys. **66**, 899 (1994).
[20]C. E. Dreyer, A. Janotti, C. G. Van de Walle, and D. Vanderbilt, Phys. Rev. X **6**, 021038 (2016).
[21]C. E. Dreyer, J. L. Lyons, A. Janotti, and C. G. Van de Walle, Appl. Phys. Express **7**, 031001 (2014).
[22]P. Ruterana, G. D. Jores, M. Laugt, F. Omnes, and E. Bellet-Amalric, Appl. Phys. Lett. **78**, 344 (2001).
[23]S. H. Wei, L. G. Ferreira, J. E. Bernard, and A. Zunger, Phys. Rev. B **42**, 9622 (1990).
[24]S. Baroni, S. De Gironcoli, A. Dal Corso, and P. Giannozzi, Rev. Mod. Phys. **73**, 515 (2001).
[25]J. Pal, G. Tse, V. Haxha, M. A. Migliorato, and S. Tomić, Opt. Quantum. Electron. **44**, 195 (2012).
[26]J. Pal, G. Tse, V. Haxha, M. A. Migliorato, and S. Tomić, Phys. Rev. B **84**, 159902 (2011).
[27]P. Y. Prodhomme, A. Beya-Wakata, and G. Bester, Phys. Rev. B **88**, 121304 (2013).
[28]K. Shimada, T. Sota, K. Suzuki, and H. Okumura, Jpn. J. Appl. Phys., Part 1 **37**, L1421 (1998).